PAPER • **OPEN ACCESS**

Influence of defects of nanostructured ZnO films on the photovoltaic characteristics of perovskite solar cells

To cite this article: D A Afanasyev *et al* 2018 *IOP Conf. Ser.: Mater. Sci. Eng.* **289** 012001

IOP Conf. Series: Materials Science and Engineering **289** (2018) 012001 doi:10.1088/1757-899X/289/1/012001

Influence of defects of nanostructured ZnO films on the photovoltaic characteristics of perovskite solar cells

D A Afanasyev[1], K Yu Mirzoev[2] and N Kh Ibrayev[3]
[1]Acting Director, Institute of Applied Mathematics, Karaganda, Republic of Kazakhstan
[2]Student, Karaganda State University named after E.A. Buketov, Karaganda, Republic of Kazakhstan
[3]Professor, Karaganda State University named after E.A. Buketov, Karaganda, Republic of Kazakhstan
E-mail: a_d_afanasyev@mail.ru

Abstract. The influence of the defects in ZnO films on the electrical and photovoltaic properties of perovskite solar cells was investigated in the work. According to the results of the research it was established that the defects in ZnO films affects the concentration of defects of perovskite films synthesized on the ZnO surface. However, the difference in the defect concentration in perovskite films is about 30%, while the concentration of defects in ZnO differs by 1000 times. A less significant influence is the concentration of ZnO defects on the electrical and photovoltaic properties of perovskite solar cells. The magnitude of the short-circuit photocurrent and the open voltage of the cells are affected by the concentration of perovskite defects and the quality of the perovskite-ZnO interface.

1. Introduction

At present, researchers are increasing attention to obtaining and studying the properties of nanostructured materials [1]. This interest is due to the great possibilities of practical application of such materials for the creation of elements of molecular electronics [2], optoelectronics [3], photovoltaic cells [4]. One of the promising materials on the basis of which it is possible to obtain various nanostructures is zinc oxide [5]. In a family of wide-band semiconductors, ZnO is a promising semiconductor in connection with the possibility of its use in the creation of various components of electronic equipment. ZnO is a recognized material for the creation of highly efficient light sources and receivers operating in the blue and ultraviolet range of the spectrum, solar cells, transparent contacts, ultrafast scintillators, gas sensors, etc. [6]. On the basis of ZnO films it is proposed to make perovskite solar cells (PSC). The basis of these cells is organo-inorganic compounds of the composition $OrPbX_3$, where Or - cation-organic compounds, such as, methylammonium, ethylammonium, etc., X – halogens Br, I, Cl. During the period from 2009 to 2014 PSC have increased their efficiency from 3.8% to more than 19% [7]. At the same time, the intensive growth of the efficiency of PSC continues [8]. Many properties of organo-inorganic perovskite materials have not been studied in detail and require further research. The degree of influence of the metal oxide film (TiO_2, ZnO, Al_2O_3), on the surface of which the perovskite films are synthesized, on the properties of solar cells remains little investigated. In this paper, the effect of defects of nanostructured ZnO films and perovskite films on the photovoltaic and electrical characteristics of perovskite solar cells with composition of ZnO-$CH_3NH_3PbI_3$-spiro-OMeTAD.

2. Experimental details

Initially, nanostructured ZnO films were fabricated by pulsed electrochemical synthesis and hydrothermal methods. The procedure of the synthesis of films is described in detail in [9].

Pulsed electrochemical deposition of ZnO nanorods was carried out in a three-electrode electrochemical cell with an aqueous electrolyte containing $NaNO_3$ and $Zn(NO_3)_2$ at a temperature of t = 70°C without mechanical stirring of the solution. Glass substrates coated with transparent electrically conductive layers of fluorine-doped tin oxide (FTO) from Sigma-Aldrich were used as a substrate. The opposite electrode was a graphite rod, and the reference electrode was a saturated Ag/AgCl electrode.

The rectangular potential pulses were applied to the substrate-cathode, the lower limit of which was U_{off} for the samples was – 0.8 V, the upper limit of U_{on} was – 1.4 V (the potentials are given relative to Ag/AgCl). The pulse rate was 2.5. The pulse frequency f was kept constant and equaled 2 Hz [10].

The synthesis of ZnO nanorods by the hydrothermal method consisted of two stages. The first stage is the deposition of a seed layer and the second stage is the synthesis of nanorods on a substrate with a seed layer of hydrothermal deposition. Zinc acetate ($Zn(CH_3COO)_2 \cdot 2H_2O$, Sigma Aldrich) and monoethanolamine (C_2H_7NO, Sigma Aldrich) used for synthesis of the seed layer ZnO The reagents were sequentially dissolved in isopropyl alcohol. The solution was applied to a pre-cleaned glass substrate coated with a FTO conductive layer by spin-coatingю This procedure was repeated 4 times. Further, to form the ZnO structure, the substrates were annealed in a muffle furnace at a temperature of 450 °C. Arrays of ZnO nanorods were synthesized on FTO substrates with a previously deposited seed layer of ZnO from an equimolar aqueous solution of zinc nitrate ($Zn(NO_3)_2$, Sigma Aldrich) and urotropine ($C_6H_{12}N_4$, Sigma Aldrich) for 10 hours. After every 2 hours samples were washed in deionized water and after the completion of the synthesis, the grown ZnO arrays were repeatedly washed in deionized water, dried and annealed at 400 °C [11].

For the synthesis of perovskite films, solutions of PbI_2 and CH_3NH_3I were used. The perovskite film $CH_3NH_3PbI_3$ ($MAPbI_3$) was deposited in two stages. In the first stage, PbI_2 was applied using the spin-coating method. The substrate was then dried at temperatures of 50 °C and 100 °C. In the second stage, a solution of ammonium methyl iodide CH_3NH_3I was applied to the sample. Later on, the perovskite film was annealed. The procedure for the synthesis of films is described in detail in [12]. All operations related to the synthesis of perovskite films were carried out in a box with an inert atmosphere (SPEKS GB 03-2M).

The morphology of the films was examined on an electron scanning electron microscope (SEM) with a field emission of Mira 3 (TESCAN). The absorption spectra of the films were recorded using a Cary 300 (Agilent) spectrophotometer. The fluorescence spectra were measured on a Cary Eclipse (Agilent) spectrofluorimeter. The kinetics of fast fluorescence of samples was measured with a pulsed spectrofluorometer with a picosecond resolution and recording in a time-correlated photon count (Becker & Hickl). Fluorescence excitation of the samples was carried out with a pulsed semiconductor laser with a λ_{gen} = 640 nm generation wavelength with – full width at half maximum (FWHM) τ = 80 ps.

Curent-voltage characteristics (CVC) were measured for PSC. The CVC of the cells was measured on Keithley 2400 instrument under standard simulated solar radiation AM 1.5, 100 mV/cm^2 (PET PHOTO Emission TECH., INC.) The electrical transport properties of PSC were studied using the method of electrochemical impedance spectroscopy. The impedance measurements were carried out under the standard simulated solar radiation AM 1.5, on the impedance meter Z-500PRO (Elins).

3. Discussion of results

The microstructure of synthesized ZnO films is shown in Figure 1. For the film obtained by the hydrothermal method, the average diameter of the rods was 150 nm. When using electrochemical synthesis, the average diameter of the rods was 660 nm. In the case of the hydrothermal method, the size of the rods is smaller than the size of the rods obtained by the electrochemical method. The rate of film synthesis is higher for the electrochemical method.

Spectra of absorption and luminescence were measured for ZnO films. The absorption spectra of ZnO are shown in Figure 2*a*. The optical density (*D*) of films obtained by different methods, and measured at 380 and 800 nm, has similar values. In the blue-green part of the spectrum, D of the films is significantly different. The luminescence spectra of the samples were also measured (Figure 2*b*). To determine the crystallinity of ZnO nanostructures, the ratio of the amplitude of the maximum intensity of the luminescence band in the visible region (I_{BO}) to the amplitude of the maximum of the edge luminescence band in the short wave region of the I_{UV} is often compared [13]. The I_{BO}/I_{UV} ratio for the electrochemical film was 2.6, and for the hydrothermal film 0.13. Therefore, the concentration of defects in ZnO nanorods obtained by the electrochemical method is much larger than the ZnO film obtained by the hydrothermal method. Indirect evidence of a high concentration of defects in the ZnO film obtained by the electrochemical method is the shape of the absorption curve 2 shown in Figure 2*a*. The film has a higher *D* value in the range of 400 to 800 nm.

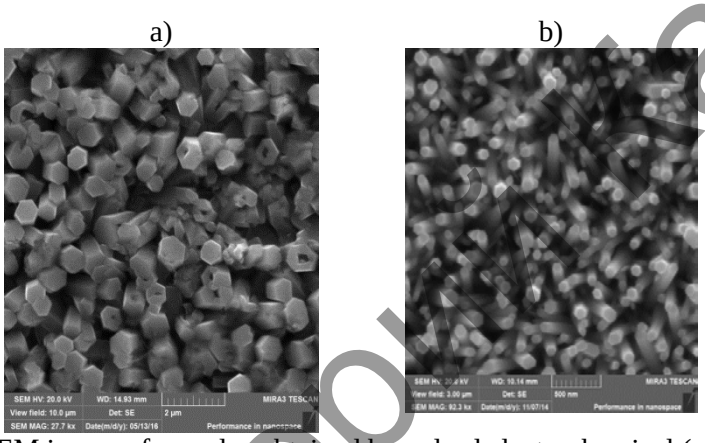

Figure 1. SEM image of samples obtained by pulsed electrochemical (*a*) and hydrothermal methods (*b*).

The concentration of defects in the films was estimated for ZnO samples. For the ZnO film obtained by the hydrothermal method on a non-conducting substrate, the resistivity of the sample and the Hall effect were measured. From the data obtained, the concentration of charge carriers in the sample was determined. Proceeding from the fact that the width of the forbidden ZnO band is high and at room temperature the contribution of the thermally activated intrinsic conductivity is small in comparison with the contribution of charge carriers from the defective levels of ZnO, the defect concentration in the film was estimated as ~ 3×10^{14} cm^{-3}. From the measurements of the resistivity of the ZnO film obtained by the electrochemical method, the concentration of defects in ZnO (electrochem. synthesis) was estimated by comparison with the specific resistance of the ZnO film (hydrothermal synthesis). This concentration was ~ 3×10^{17} cm^{-3}. Thus, the estimation of the defect concentration in ZnO films in electrical measurements agrees qualitatively with the data obtained from measurements of the luminescent properties of the samples.

The perovskite film had a granular structure with a granule size of the order of 100 nm. For the formation of films with hole conductivity, solutions based on Spiro-OMeTAD (N^2, N^2, $N^{2'}$, $N^{2'}$, N^7, N^7, $N^{7'}$, $N^{7'}$-octakis (4-methoxyphenyl) - 9, 9'-spirobi [9H-fluorene] - 2, 2', 7,7'-tetramine) in chlorobenzene were prepared. After the application of the film with hole conductivity, a silver electrode 60…100 nm thick was deposited in a vacuum (10^{-6} torr) using a thermal evaporation method, the deposition rate being 1.5 Å/s.

Figure 3 shows a section of a perovskite cell based on nanostructured ZnO (hydrothermal synthesis), including spiro-OMeTAD and a silver electrode. The total thickness of the sample with ZnO nanostructures (hydrothermal synthesis) was approximately ~ 1360 nm, of which ~ 1054 nm the thickness of the ZnO layer together with perovskite, the thickness of the spiro-OMeTAD film ~ 243 nm and Ag thickness ~ 60 nm. The thickness of the perovskite film without ZnO is 400 nm. For the

PSC with ZnO, obtained by the electrochemical method, the thickness was about ~ 1300 nm, of which ~ 600 nm the thickness of the ZnO layer, the thickness of the perovskite ~ 600 nm, the thickness of the spiro-OMeTAD film ~ 200 nm, and the thickness of Ag ~ 100 nm.

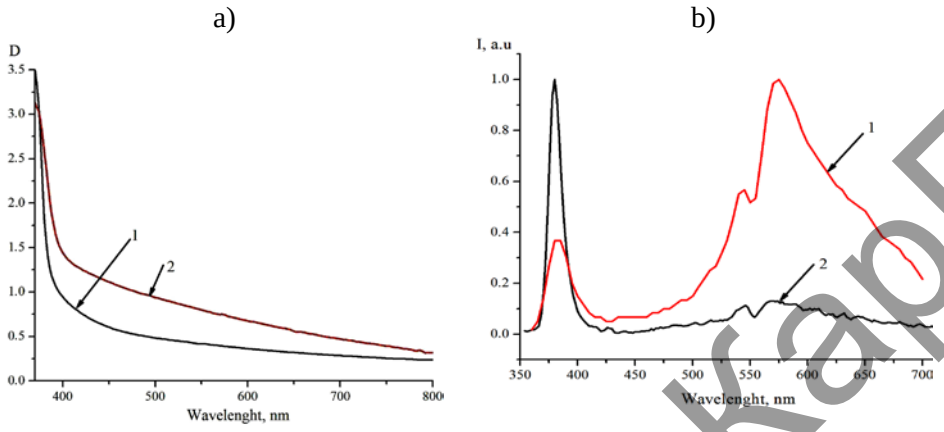

Figure 2. Absorption spectra (*a*) and luminescence (*b*) of ZnO nanorods obtained by pulsed electrochemical (1) and hydrothermal (2) methods.

Figure 3. Perovskite cell based on ZnO nanostructures, hydrothermal synthesis.

The absorption spectra of $CH_3NH_3PbI_3$ ($MAPbI_3$) films are shown in Figure 4 (curves 1–3). The shape of the curves indicates the formation of a perovskite film. However, the form of the dependence of the absorption coefficient D on the wavelength indicates that the perovskite films have different qualities depending on which substrates for making $MAPbI_3$ were used. The absorption spectrum of a perovskite film based on hydrothermal ZnO rods differs significantly from the absorption spectra of perovskite films obtained on other ZnO coating (Figure 4*a*). Additional information can be obtained from the luminescence spectra.

The luminescence spectra of the $MAPbI_3$ films are shown in Figure 4*b*. For the samples obtained, the ratio of the luminescence intensity to the optical density of the film at a wavelength of 470 nm ($I_{MAX}/ D_{470\ nm}$) was estimated. These ratios are given in Table 1. The maximum ratio is observed for the perovskite film obtained on the ZnO surface (hydrothermal synthesis). The lowest value is observed for the ZnO film, (electrochem. synthesis). Thus, the perovskite film on the ZnO surface (the hydrothermal method) has less concentration of defects than the rest of the films. Large concentration of defects in ZnO is observed for perovskites on the surface of ZnO (electrochem. synthesis).

To study the effect of the properties of compact ZnO films on the efficiency of charge transfer in a perovskite film ($MAPbI_3$), the kinetics of the luminescence of perovskite films in the nanosecond time range was studied. The kinetics of the luminescence of films contains the stage of increase and quenching of the luminescence intensity. After the laser excitation is completed, the luminescence of the perovskite film is increased. The time after the end of laser excitation to the maximum of the luminescence intensity is in the range from 0.7 ns to 1.5 ns (Table 1). Then the luminescence intensity

falls. In the case of the sample $CH_3NH_3PbI_3$ on the surface of the FTO film, the luminescence kinetics has an exponential form of damping, the lifetime is 22.3 ns. In the case of the $MAPbI_3$ film on the surface of the ZnO film, the luminescence lifetime decreases. For different ZnO films, the lifetime is different: $\tau_{hydrothermal.}$ = 17.2 ns; $\tau_{electrochym.}$ = 22.3 ns.

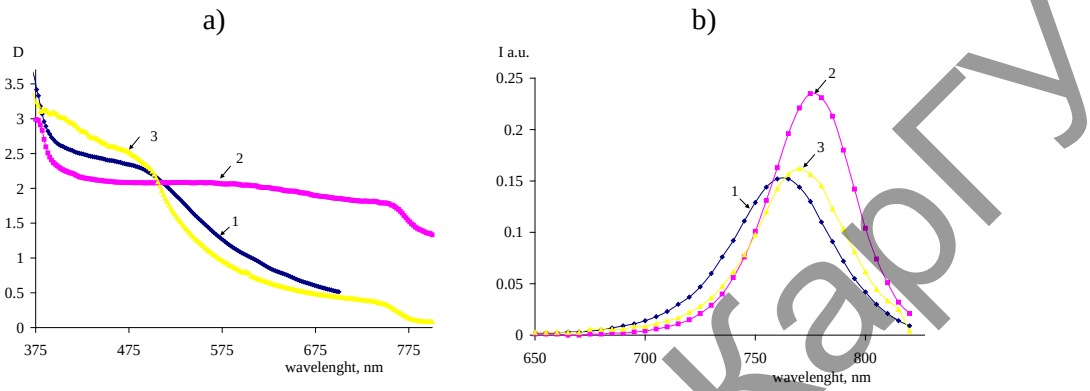

Figure 4. Absorption *(a)* and luminescence spectra *(b)* of $MAPbI_3$ films obtained on the ZnO surface: 1) FTO; 2) ZnO nanorods, hydrotherm. synthesis; 3) ZnO nanorods, pulsed electrochem. method.

Table 1. Luminescent characteristics and effect of n-type and p-type layers on suppression of luminescence of perovskites.

Sample	$I_{MAX}/D_{470\ nm}$	$k\ (I_{MAPbI3}/I_{MAPbI3\text{-}spiro\text{-}OMeTAD})$	$k\ (\tau_{MAPbI3}/\tau_{MAPbI3\text{-}spiro\text{-}OMeTAD})$	Time of increase of luminescence intensity Δt, (ns)
FTO–perovskite	0.065	15.2	3.19	1.53
ZnO (electrochem.) - perovskite	0.064	2.35	3.46	1.34
ZnO (hydrothermal) perovskite	0.113	2.07	1.69	0.7

As is known, the efficiency of charge transfer can be estimated by quenching the intensity or lifetime of luminescence [14]. Analysis of the data shows that the best charge transfer is observed for the perovskite–ZnO sample (hydrothermal synthesis) (Table 2). For the perovskite-ZnO sample (electrochem. synthesis), charge transfer proceeds less intensively. The effect of the spiro-OMeTAD film on the intensity and lifetime of the luminescence of perovskite films. The luminescence intensity of $MAPbI_3$ is quenched less than the decrease in the lifetime of the perovskite luminescence. This is due to a more efficient electron transfer in the samples of the perovskite-nanorods ZnO. The short rise time of the luminescence in the perovskite-ZnO film (hydrothermal synthesis) indicates a high carrier transport velocity in this sample. In the case of the ZnO sample (electrochem. synthesis)–$MAPbI_3$–Spiro-OMeTAD, the maximum rate of hole transport from perovskite to the Spiro-OMeTAD layer is observed. A higher rate of hole transport is an indirect indication of a lower rate of electron transfer from perovskite layer to ZnO.

For perovskite films, it is possible to estimate the concentration of defects in accordance with the method described in detail in [15, 16] when photoexcitation of a sample by a short laser pulse with low energy (where Auger recombination can be neglected) and assuming that the recombination of trap states is much slower, than edge radiative recombination. The initial concentration of charge carriers after photoexcitation $n_c(0)$ can be defined as:

$$n_C\,(0) = \frac{\sum_i n_{TR}^i(0)\left(1-e^{-a_i\tau_0\frac{I_{PL}}{k}}\right)}{k} \quad (1)$$

where $n_{TR}^i(t)$ is the trap state density and a_i is the parameter related to the capture cross section and the velocity of the charge carriers. Assuming that the ratio between the integrated photoluminescence intensity (I_{PL}) of the band ($I_{PL} = k\left(\int_0^\infty n_C(t)\Big/\tau_o dt\right)$, where k is the constant), the concentration of defects in the perovskite film (n_{TR}^i) can be determined from equation 1.

Table 2. Luminescence lifetime of perovskite films.

Interface (sample, type of film, synthesis method)	Constants of electron transfer (k, ns^{-1})
$MAPbI_3$→ FTO	0.045
$MAPbI_3$→ ZnO (hydrothermal synthesis)	0.058
$MAPbI_3$→ ZnO (electrochem. synthesis)	0.045
$MAPbI_3$→ Spiro-OMeTAD (FTO), ($k_{FTO–MAPbI3\ –\ Spiro\text{-}OMeTAD}$ - $k_{FTO–MAPbI3}$)	0.098
$MAPbI_3$→ Spiro-OMeTAD, (hydrothermal synthesis)	0.040
$MAPbI_3$→ Spiro-OMeTAD, (electrochem. synthesis)	0.110

For $MAPbI_3$-ZnO samples, the dependence of the luminescence intensity of the perovskite film on the laser excitation energy was measured. To determine the trap concentration in perovskite films, plots of the luminescence intensity (I_{PL}) were plotted against the concentration of free charge carriers (n_c) (Figure 5*a*). The concentration of charge carriers was estimated on the basis of the main characteristics of laser excitation and the optical density of the perovskite film. The form of the approximating curve obtained using Equation 1 is shown in Figure 5*b*. The data obtained from the approximation of the curves for perovskite films are given in Table 3. It can be seen from the table data that a perovskite film ($MAPbI_3$) with a higher defect concentration is formed on the ZnO film with a higher defect concentration.

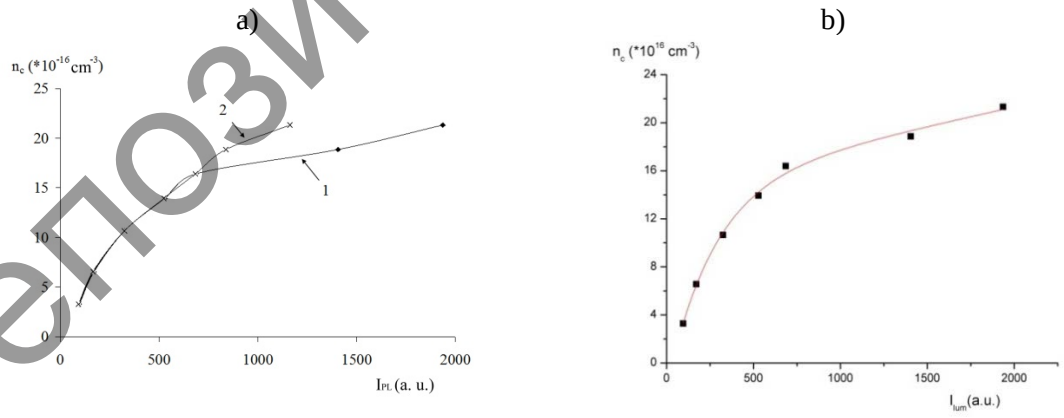

Figure 5. Determination of the trap state densities: *a)* Dependence of n_c on luminescence intensity: 1) perovskite-ZnO (electrochem. synthesis); 2) perovskite-ZnO (hydrothermal synthesis). *b)* Approximation of the experimental data using equation 1 for the perovskite–ZnO film (electrochem. synthesis).

The effect of the morphology and defect structure of ZnO on the photovoltaic properties of PSC is studied. The light and dark CVC of the perovskite cells are shown in Figure 6. The data obtained are also given in Table 4. It can be seen from the light CVC that for a solar cell with a ZnO film

(electrochem. synthesis) a higher value of the idling voltage (V_{oc}) the value of the short-circuit current (J_{sc}) as compared to a cell based on ZnO (hydrothermal synthesis). A smaller value of V_{oc} for the perovskite-ZnO sample (hydrothermal synthesis) is associated with a high recombination rate at voltages U> 0.4 V compared to cells based on ZnO (electrochem. synthesis), Figure 6*b*.

Table 3. Concentration of defects in perovskite films.

Sample (substrate)	Concentration of defects n_{tr}
Perovskite-ZnO, (hydrothermal synthesis)	1.2×10^{16} см$^{-3}$
Perovskite-ZnO, (electrochem. synthesis)	1.7×10^{16} см$^{-3}$

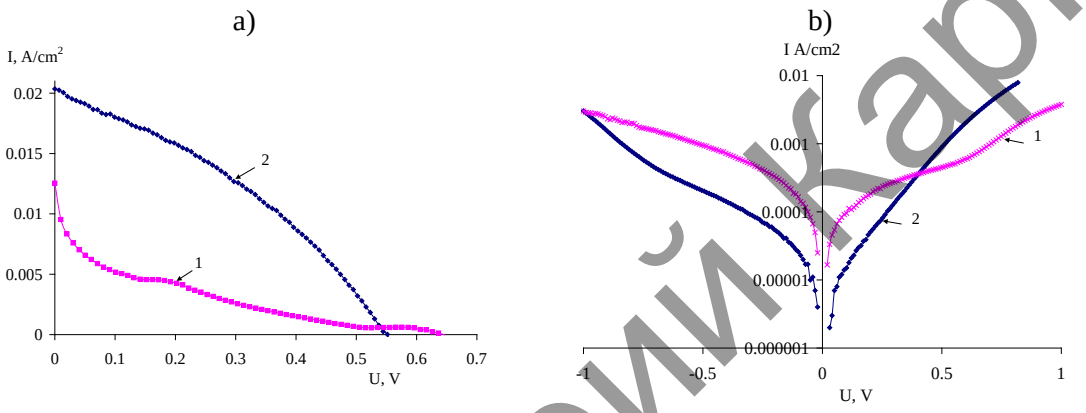

Figure 6. Light (*a*) and dark (*b*) CVC of solar cells based on nanostructured ZnO films: 1) ZnO, electrochem. synthesis; 2) ZnO, hydrotherm. synthesis.

The dark CVC of the cells are shown in Figure 6*b*. It can be seen from Figure 6*b* that for a cell with a ZnO film (electrochem. synthesis) large leakage currents are observed on the straight part of the CVC at a low voltage value of up to 0.4 V. At high voltages, the leakage currents are higher for a cell with a ZnO film (hydrotherm. synthesis). The results obtained make it possible to analyze the properties of the perovskite film and the perovskite-ZnO interface. The smaller concentration of defects in the perovskite film and the ZnO film (hydrothermal synthesis) leads to lower dark currents in the cell at low operating voltages. High leakage currents at voltages greater than 0.4 V indicate the emergence of additional channels for the recombination of charge carriers in a cell at high voltages (U> 0.4 V). In this case, no recombination losses are observed in the perovskite–ZnO film (electrochem. synthesis).

Table 4. Photovoltaic and electrical properties of perovskite solar cells.

The method of manufacturing ZnO films	J_{sc}, A/cm^2	U_{oc} B	FF	η %	R_{SER} Ом/cm^2	R_{SH} Ом/cm^2	S, cm^2
Electrochem. synthesis	0.012	0.636	0.12	1.02	327.1	51.24	0.24
Hydrothermal synthesis	0.021	0.551	0.30	3.85	35.95	82.56	0.21

The impedance of the PSC was measured. Figure 7 shows the impedance spectrum for the perovskite-ZnO cell (hydrothermal synthesis). For a more accurate determination of the recombination time characteristics in perovskite cells, the simplest model of the solar cell R1–(R2, C1) was used. The electrical schematic of the model is shown in the Figure 7. In the solar cell model, R1 is associated with the series resistance of the contacts and layers in the solar cell, R2 is related to the electrical resistance of the perovskite film, and C1 is the cell capacitance. The values of the indices of the solar cell chain were estimated. The effective lifetime was determined as (τ = $R2\times C2$). The results are shown in Table 5.

The data obtained for the cells by the method of impedance spectroscopy (Table 5) correlate with the data on the measurement of the light CVC (Table 4). The high value of the series resistance of the R_{SER} cell corresponds to the high value of R1 obtained when measuring the impedance of the cells and vice versa.

Comparison of the recombination constants shows that when the cells are illuminated, the recombination rate in a cell with ZnO (electrochem. synthesis) is 25% higher than the recombination rate in a cell with ZnO (hydrothermal synthesis). This indicates that the concentration of defects of nanostructured ZnO films does not significantly affect the rate of recombination of electron-hole pairs at the ZnO–perovskite interface. A comparison of the changes in the rate of recombination in PSC (25%) with the data of Table 3 indicate that defects in perovskite have a greater significance for recombination in PSC and that defects in ZnO films are practically unaffected.

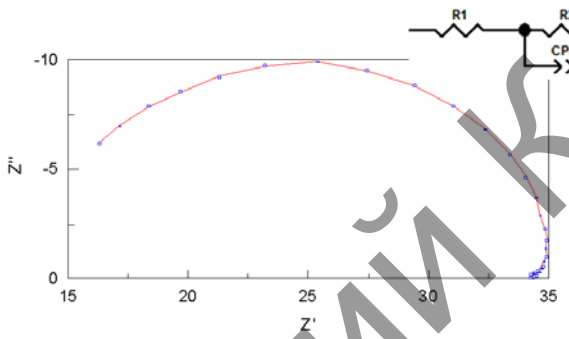

Figure 7. Nyquist plot for a solar cell based on ZnO (hydrothermal synthesis). In the inset, the model of the solar cell electrical circuit.

Table 5. The values of the elements of the chain of perovskite solar cells under illumination, in accordance with the equivalent circuit.

Solar cell with ZnO (method of synthesis)	R_1, Ω	R_2, Ω	C_1, F	n_1	τ (μs)
Hydrotherm. method	12.5	23.6	6.7×10^{-7}	0.863	15.7
Electrochem. method	178	294	4.0×10^{-8}	0.96	11.8

It is important that for ZnO films obtained by different methods, the values of the series resistance of cells significantly differ (Table 4, 5). The specific resistance of the ZnO film obtained by the electrochemical method is significantly lower than the resistance of the ZnO film obtained by the hydrothermal method. This resistance of PSC's on the basis of ZnO films (electrochem. synthesis) is an order of magnitude higher than the resistance of cells based on ZnO films (hydrothermal synthesis). This is possible if there is a high resistance at the ZnO–perovskite interface. Thus, these results indicate a significant effect of the ZnO-perovskite interface on the photovoltaic characteristics of the perovskite solar cells obtained.

4. Summary

The paper presents the results of a study of the influense of defect concentrations of nanostructured ZnO films on the electrical and photovoltaic properties of PSC. The different methods determine the concentration of defects in zinc oxide films and perovskite films. On ZnO samples with a higher defect concentration, a perovskite with a higher defect concentration is formed. However, if the concentration of defects in ZnO differs by a factor of 1000, then in perovskite films the defect concentration's differs only by 30%.

For a solar cell with a ZnO film (electrochem. synthesis), a higher value of the open circuit voltage (V_{oc}) but a smaller value of the short-circuit current (J_{sc}) is observed compared to a cell based on ZnO

(hydrothermal synthesis). The smaller value of J_{sc} is associated with a lower charge transfer rate in the $MAPbI_3$→ZnO film (electrochem. synthesis). A smaller value of V_{oc} for $MAPbI_3$-ZnO sample (hydrothermal synthesis) is associated with a high recombination rate at voltages U>0.4 V compared to cells based on ZnO (electrochem. synthesis).

A smaller concentration of defects in the perovskite-ZnO film (hydrothermal synthesis) leads to lesser dark currents in the cell. High leakage currents at voltages exceeding 0.4 V indicate the occurrence of additional recombination processes at high voltages. In this case, no perovskite-ZnO (electrochem. synthesis) of these recombination processes is observed.

Acknowledgments
This work was carried out with the financial support of the Ministry of Education and Science of the Republic of Kazakhstan.

References

[1] Ryzhonkov D I, Levina V V, Dzidziguri E L 2010 *Nanomaterials* (Moscow: Binom, Laboratoriy znanii) (In Russian)
[2] Ghosh A W 2011 *Semicond. Sci. Tech.* **5** 383–479
[3] Iwasaki Y, Osasa T, Asahi M, Matsumura M, Sakaguchi Y, Suzuki T 2006 *Phys. Rev. B.* **74** 195209 doi: 1103/PhysRevB.74.195209
[4] Ito S, Murakami T N, Comte P et al. 2008 *Thin Solid Films* **516** 4613–4619 doi: 10.1016/j.tsf.2007.05.090
[5] Djurisic A B, Leung Y H 2006 *Small* **2** 944–961 doi: 10.1002/smll.200600134
[6] Djurisic A B, Chen X Y 2010 *Progress in quantum electronics* **34** 191–259 doi: 10.1016/j.pquantelec.2010.04.001
[7] Snaith H J 2013 *J. Phys. Chem. Lett.* **4** 3623–3630 doi:10.1021/jz4020162
[8] Best Research-Cell Efficiencies [Electronic resource] URL: https://www.nrel.gov/pv/assets/images/efficiency-chart.png
[9] Afanasyev D A, Aitymov Zh K, Ilyassov B R et al. 2017 *Bulletin of the Karaganda-physics* № 1(85) 22–27
[10] Klochko N P, Khrypunov G S 2012 *Semiconductor* **46** 825–831 doi: 10.1134/S1063782612060127
[11] Ilyasov B R, Ibrayev N Kh, Nuraje N 2015 *Materials Science in Semiconductor Processing* **40** 885–889 doi: j.mssp.2015.07.087
[12] Ibrayev N Kh, Afanasyev D A, Mirzoev K Yu, Smagulov G K 2016 *Eurasian physical technical journal* **13** 45–51
[13] Li D, Leung Y H, Djurisic A B et. al. 2004 *Applied Physics Letters* **85** 1601–1603 doi: 10.1063/1.1786375
[14] Pydzin´ska K, Karolczak J, Kosta I et. al. 2016 *ChemSusChem* **9** 1647–1659 doi: 10.1002/cssc.201600210
[15] Xing G, Mathews N, Lim S S et. al. 2014 *Nature materials* **13** 476 – 480 doi: 10.1038/nmat3911
[16] Peng W, Anand B, Liu L et. al. 2016 *Nanoscale* 8 1627–1634 doi: 10.1039/C5NR06222E